SPACE CHARGE ANALYSIS ON THE MULTI-WIRE PROPORTIONAL CHAMBER FOR THE HIGH RATE INCIDENT BEAMS

Ken KATAGIRI, Takuji FURUKAWA, Eri TAKESHITA, and Koji NODA
National Institute of Radiological Sciences, Chiba, Japan

Abstract

A transient gain reduction process of the multi-wire beam profile monitor was numerically investigated for the detailed design of geometric parameters. In order to consider the space-charge effect, we developed a numerical code based on the drift-diffusion model. To find the relations between the gain reductions of the output signal and the space-charge distributions, the calculations were performed for the time period of $\sim 10 - 100\,\mu$s, which is much longer than the time required by ions to travel from the anode to the cathode. We found the ion distributions to be quasi-stationary for the successive beam injection of $\sim 10^8 - 10^9$ pps.

INTRODUCTION

In the 3D irradiation system with pencil beam scanning, which are under planning at HIMAC [1], the information from the MWPC is going to be used for the fluence distribution measurement of the 3-D dose reconstruction method [2]. In the case of high rate irradiation ($\sim 10^8 - 10^9$ pps), a gain reduction of the output signal has been observed so far in the scanning beam experiment at HIMAC. If the gain reduction is much larger, the fluence distribution measured by the MWPC is expected to differ from the actual beam profile. Therefore, the improvement of the MWPC to decrease the gain reduction is important issue.

The gain reduction of the wire chamber in pulse mode operation is explained by the ions around the anodes [3, 4]. On the other hand, the space charge distribution in the beam monitor, which is employed as the current mode operation, have not been investigated in detail. In order to investigate the relations between the gas gain variation and the temporal evolution of ion distribution, we have developed a numerical code based on the drift-diffusion model for electrons and ions. A helium-filled MWPC chamber was modeled to be a simple geometry including three anode wires and two cathodes. To take into account the effects of the ion motion on the space-charge effect, the time period to be considered in the calculation was extended much longer than the time required by ions to travel between electrodes. The incident beams with constant irradiation rate were considered by a simple model using a W-value. The gas gain was evaluated from the output signal, which is calculated by the conservation of the electrons. In this paper, we present the simulation results of the relations between the gas gain variation and the temporal evolution of ion distribution.

SIMULATION MODEL

Governing equations

Two dimensional analysis was performed to simulate the motion of charged particles in a complicated potential field, which is distorted by the space charge effect. The pressure and the temperature in a He-gas filled chamber were assumed to be 10^5 Pa and 300 K, respectively. In order to simplify the analysis, particles of electrons (e^-) and positive ions (He^+) were only taken into account. Under the drift-diffusion approximation, the ion and electron fluxes are represented as follows:

$$\boldsymbol{\Gamma}_\mathrm{s} \equiv n_\mathrm{s}\boldsymbol{u}_\mathrm{s} = -D_\mathrm{s}\nabla n_\mathrm{s} \pm n_\mathrm{s}\mu_\mathrm{s}\boldsymbol{E}. \quad (1)$$

Here, $\boldsymbol{\Gamma}_\mathrm{s}$ is the particle flax, n_s the density, $\boldsymbol{u}_\mathrm{s}$ the drift velocity, D_s the diffusion coefficient, μ_s the mobility, and subscript s is the particle species (e: electron, i: ion). Particle conservations for electrons and ions are expressed by the continuum equation:

$$\frac{\partial n_\mathrm{s}}{\partial t} + \nabla \cdot \boldsymbol{\Gamma}_\mathrm{s} = G - L. \quad (2)$$

Here, G and L are the generation and loss term, respectively. The generation term was derived by using Townsend first ionization coefficient α:

$$G = \alpha n_\mathrm{e}|\boldsymbol{u}_\mathrm{e}|. \quad (3)$$

The radiative recombination, and the three body recombination were included as recombination processes:

$$L = \alpha_\mathrm{RR} n_\mathrm{e} n_\mathrm{i} + \alpha_\mathrm{3BR} n_\mathrm{e}^2 n_\mathrm{i}. \quad (4)$$

Here, α_RR and α_3BR are the rate coefficient for the radiative recombination and the three body recombination, respectively.

The swarm parameters (α, μ_s) and the diffusion coefficient D_s were evaluated as a function of the electric field $|\boldsymbol{E}|$ under the local field approximation (LFA). For these parameters, the Poisson equation was concurrently solved:

$$\nabla^2\phi = -\frac{e(n_\mathrm{i} - n_\mathrm{e})}{\varepsilon_0}, \quad (5)$$

$$\boldsymbol{E} = -\nabla\phi. \quad (6)$$

The diffusion coefficient for ions D_i was derived from the Einstein's formula. The diffusion coefficient for electrons D_e was evaluated by using the BOLSIG+ [5], which is the Boltzmann equation solver. The Townsend first ionization coefficient α, and mobility μ_s, were derived from the Siglo Data Base. [1]

[1] The Siglo data base, CPAT and Kinema Software, http://www.siglokinema.comi.

Numerical method

From the Eq. (1) and Eq. (2), we obtain the advection diffusion equations as follows:

$$\frac{\partial n_s}{\partial t} \pm (\mu_s \boldsymbol{E} \cdot \nabla) n_s = \mp n_s (\nabla \cdot \mu_s \boldsymbol{E}) + D_s \nabla^2 n_s + G - L. \quad (7)$$

To calculate the advection terms in Eq. (7), we employed the M-type CIP (Constrained Interpolation Profile) method [6]. For the time integrations of the non-advection terms in Eq. (7), we also used the 2nd order Runge-Kutta method. We employed the Red-Black SOR (Successive Over Relaxation) method for the calculation of Eq. (5). In order to reduce the calculation load of Eq. (5), the potential distribution of ϕ^{n-1}, which is the results at previous time of $t = n - 1$, was used as an initial value for the calculation of ϕ^n. To interpolate the Siglo data base, and data tables obtained by the BOLSIG+, we used the cubic spline method.

Fig. 1(a) shows a schematic diagram of the MWPC in a discrete space. For the representation of the multi-wire geometry, we used a rectangular grid. The region of 6×6 mm square was discretized by the staggered grid (Arakawa-B grid). Three wires were represented to be 1×1 rectangular grids (30×30 μm). The outlet boundary condition was applied to the surface of the two cathodes at y=−3 and 3, and to the surface of the three anodes. The periodic boundary condition was also applied to the boundaries at x=−3 and 3.

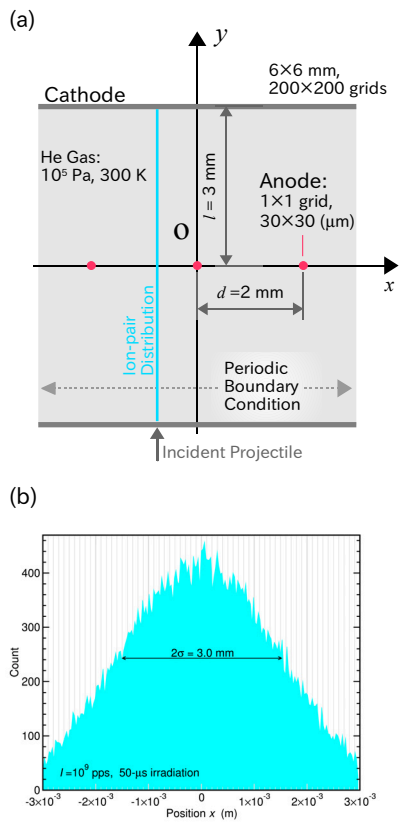

Figure 1: (a) Schematic diagram of the MWPC configuration. (b) The staggered grid (Arakawa-B grid).

The projectiles were injected with the constant irradiation rate of $I = 10^7 - 5 \times 10^9$ pps. The beam profile formed by whole projectiles was determined to be a gaussian distribution of 2σ =3.0 mm, as shown in Fig. 1(b). The beam profile along the z-axis was assumed to be homogeneous in the depth of $\Delta z_{\rm profile}$=3 mm. The ion-pairs produced by an incident projectile were distributed as the density value in a column parallel to the y-axis, as shown in Fig. 1(a). The number of initial ion-pairs $N_{\rm init}$ is simply given by

$$N_{\rm init} = \Delta E / W, \quad (8)$$

where, ΔE is the Energy loss of the projectile in $y = -6 - 6$ mm, and W is the W-value for helium gas. Assuming a 350-MeV/u ^{12}C ion injected into the 1-atm helium gas (ΔE=1.18×10^4 eV), the number of initial ion-pairs was estimated to be $N_{\rm init} = 278$ by using the W-value of $W = 42.4$ eV.

The output signal i was evaluated as the total value of the three wires by using a conservation relation of the electrons:

$$i^n\,[\mathrm{s^{-1}m^{-1}}] = \left\{ \left(\int n_e^{n-1} dS + \int G \Delta t\, dS - \int L \Delta t\, dS \right) - \int n_e^n dS \right\} / \Delta t. \quad (9)$$

Here, superscript n denotes the index of time, and Δt is the time step ($= t^n - t^{n-1}$) . The spatial integrations were performed over the whole region (6 × 6 mm). By means of the output signal i, the gas gain M was evaluated as follows:

$$M^n = \frac{i^n}{N_{\rm init}(I/\Delta z_{\rm profile})}. \quad (10)$$

RESULTS AND DISCUSSION

Fig. 2 shows the comparison of the gas gain obtained from numerical calculation with the theoretical curve. The theoretical curve was evaluated by integrating the Townsend first ionization coefficient α along the y-axis. In this numerical calculation, the space charge effect was not considered to be consistent with the theoretical curve. Although there are differences of ≃10%, the numerical results near to the theoretical curve. We confirmed that our code is capable of quantitative estimation of the gas gain. The differences between the numerical results and the theoretical curve are due to the error of the electric field around the anodes, which is caused by the discrete grids.

Temporal evolution of ion distribution is shown in Fig. 3 for $I = 10^9$ pps. We see that the ions move basically along the lines of the electric force. The ions arrive at the cathodes at $t \simeq 20\,\mu$s. We confirmed that the ion distribution

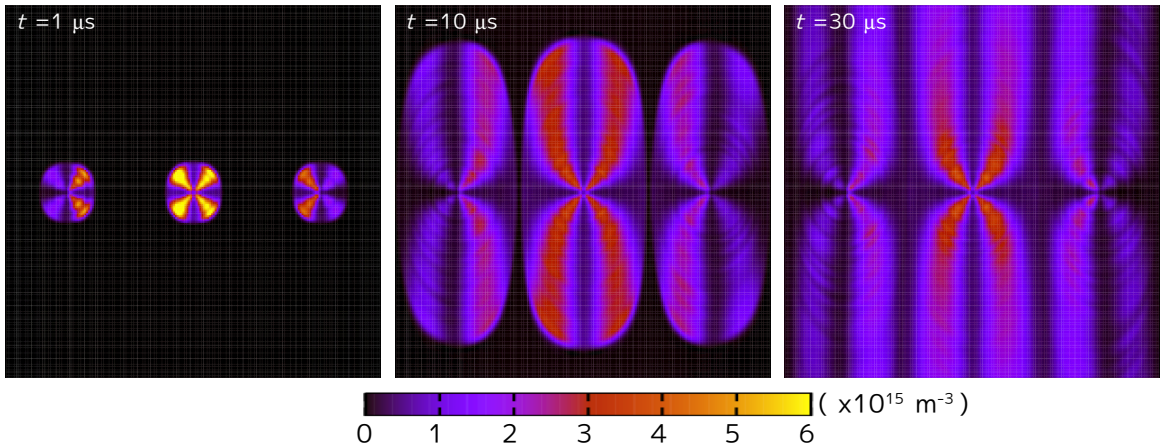

Figure 3: Temporal evolution of ion distribution for applied voltage of $V = 900$ V, irradiation rate of $I = 10^{9}$ pps.

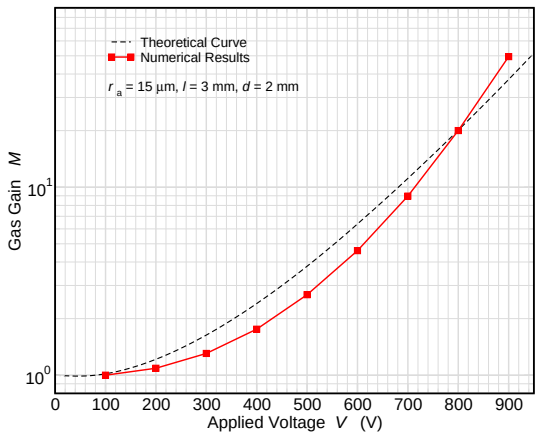

Figure 2: Comparison of the gas gain obtained from numerical calculation with the theoretical curve.

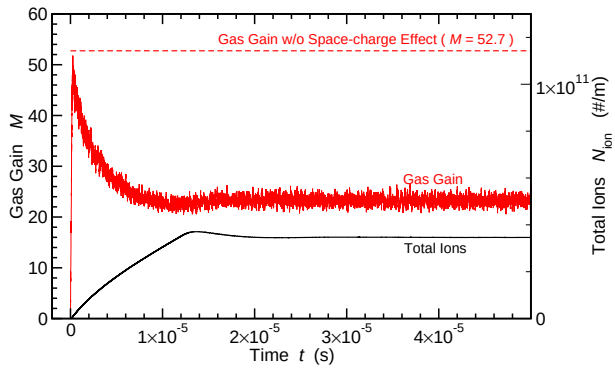

Figure 4: Temporal evolution of the Gas gain M for applied voltage of $V = 900$, irradiation rate of $I = 10^{9}$ pps.

was established to be stationary after the arrival of ions, as shown in the figure of $t = 30\,\mu$s. The ion densities on the lines of $x = -2, 0, 2$ and $y = 0$ mm are relatively low due to the potential ridge. For the stationary ion distribution established after $t \simeq 20\,\mu$s, the electric field around the center anode was decreased by $\simeq 11\%$ (3.5×10^{6} V/m $\rightarrow$ 3.1×10^{6} V/m).

Fig. 4 shows the temporal evolutions of the gas gain for $I = 10^{9}$ pps. The temporal variation of the number of total ions ($= \int n_{\rm i}\, dS$ [m^{-1}]) is also plotted as a reference. The number of total ions turns to be constant when the ions arrive at the cathodes ($t \simeq 20\,\mu$s). Due to the reduction of the electric field mentioned above, the gas gain is drastically decreased during about $10\,\mu$s from the beam injection beginning ($t = 0$ s). After $20\,\mu$s from $t = 0$ s, the gas gain begins to be almost constant. We found that this time corresponds to the beginning of the equilibrium of the number of the total ions.

CONCLUSION

We confirmed that the calculation code has capability to estimate the gas gain quantitatively. The gas gain was reduced by the space charge effect for the successive beam injection. We found that the transient gas gain begin to be constant by the quasi-stationary ion distribution. In order to examine further the capability of the quantitative estimation on the gas gain, this output signal needs to be compared with the results obtained by the beam experiments at HIMAC.

REFERENCES

[1] T. Furukawa, T. Inaniwa, et al., Med. Phys., **34**, (2007), 1085.

[2] T. Furukawa, N. Saotome, et al., Med. Phys., **35**, (2008) 2235.

[3] Glenn F. Knoll, *Radiation Detection and Measurement* (Wiley, New York, 2000).

[4] T. Sakae, A. Nohtomi, Nucl. Instrum. and Meth. A, **397** (1997) 323 .

[5] G.J.M. Hagelaar and L.C. Pitchford, Plasma Sources Sci. Technol. **14** (2005) 722.

[6] T. Yabe, T. Aoki, Comput. Phys. Comm., **66** (1991) 219.